Desalination and Water Treatment
www.deswater.com

doi: 10.5004/dwt.2018.22319

118 (2018) 304–313
June

Removal of direct dyes from aqueous solution by adsorption onto the mangrove charcoal activated by microwave-induced phosphoric acid

Nguyen Van Suc

Ho Chi Minh City University of Technology and Education, 01 Vo Van Ngan, Thu Duc, Ho Chi Minh City, Vietnam, email: sucnv@hcmute.edu.vn

Received 16 October 2017; Accepted 5 April 2018

ABSTRACT

This study describes the enhanced adsorption capacity of modified mangrove charcoal (MMC) using microwave irradiation with the diluted acid H_3PO_4 for removal of direct dyes including direct yellow 132, direct blue 71, and acid blue 193 from aqueous solution. Affecting parameters such as pH, contact time, and temperature were investigated. Results showed that the adsorption of direct dyes was favorable at acidic conditions and at 100 min contact time to reach the adsorption equilibrium. Adsorption kinetic study suggested that the adsorption process of direct dyes onto MMC was well described via pseudo-second-order model. For equilibrium thermodynamic studies, it was found that the adsorption process followed the Freundlich isotherm model. Thermodynamic studies indicated that adsorption reaction of direct dyes onto MMC was an endothermic and spontaneous process.

Keywords: Direct dyes; Mangrove charcoal; Microwave irradiation; Adsorption kinetics; Adsorption isotherms

1. Introduction

Textile industry is one of the most important sources of income in developing countries. For example, Vietnam, the export value of its textile industry in 2016 accounts for 11.515% of its gross domestic product, second largest in the country [1]. This, however, comes together with a large-scale environmental challenge due to the amount of wastewater generated in the process. It has been documented that the textile sector per year consumes thousand tons of chemicals and generated billion cubic meters of wastewater containing significant amount of residue dye and chemicals. All of this could accumulate the environment, and potentially, be converted into more toxic compounds and cause harmful effects in human. Ideally, all of the wastewater should be treated completely before being discharged into the environment; however, given the enormous scale, and the complexity, it is still a complex challenge. Not only at very large scale, but also wastewater from textile industry contains high color intensity dyes and has high chemical oxygen demand that are quite difficult to treat within a reasonable economic terms.

Many methods have been studied to remove color from the textile wastewater, including coagulation/flocculation [2–4], electrocoagulation [5–7], membrane filtration [8,9], and adsorption [10–12]. Among these, adsorption has the economic appealing because of its relatively simple process which requires low capital investment and operation cost, especially if inexpensive adsorbents can be identified.

With this driver, low-cost materials such as adsorbents derived from biosources have been intensively studied for use in the adsorption to remove contaminants from wastewater, including dyes from the textile wastewater [13–16]. By utilizing effectively, this can also be a value-added to the often abundant by-products from local agriculture sector. In this research, the focus is on the possibility of using charcoal material from mangrove wood, a popular material in Vietnam, as a candidate for the adsorption process of removal of direct dyes from aqueous solution. This charcoal is produced by dried distilling the mangrove wood, and used exclusively as fuel for cooking. The charcoal cannot be used directly in adsorption because of the dried distilling which is conducted at low temperature, resulting in a large

* Corresponding author.

amount of organic residues which makes it and become an ineffective adsorbent. Further treatment to convert this into activated carbon has been shown to improve its adsorption properties; for example, treating with acid or alkaline at high temperature in the atmosphere of N_2. However, the available methods often require expensive equipment, using extensive energy and chemicals, which can reduce the overall environmental value of the charcoal. In our method, the mangrove charcoal (MC) was irradiated by microwave for short time in the presence of the diluted phosphoric acid. This modification process is simple, uses fewer chemicals, and can be conducted using available household microwave ovens. The adsorbent prepared by this method was employed to study the adsorption process of direct dyes in aqueous solutions, including kinetics and adsorption equilibrium. These data were used to calculate the dimension of single-stage adsorption batch reactor to achieve specific adsorption efficiency.

2. Experimental

2.1. Materials and methods

All chemicals used in this work were of analytical grade from Sigma-Aldrich. Three type of dyes were direct yellow 132 (MF: $C_{27}H_{22}N_6Na_2O_9S_2$; MW: 684.61), direct blue 71 (MF: $C_{40}H_{23}N_7Na_4O_{13}S_4$; MW: 1,029.87), and acid blue 193 (MF: $C_{20}H_{13}CrN_2NaO_5S$; MW: 468.3785). Chemical structures of these dyes are shown in Fig. 1. The stock of dye solutions was prepared by dissolving 0.1 g of each dye in 100 mL of distilled water. Working solutions at specific concentrations

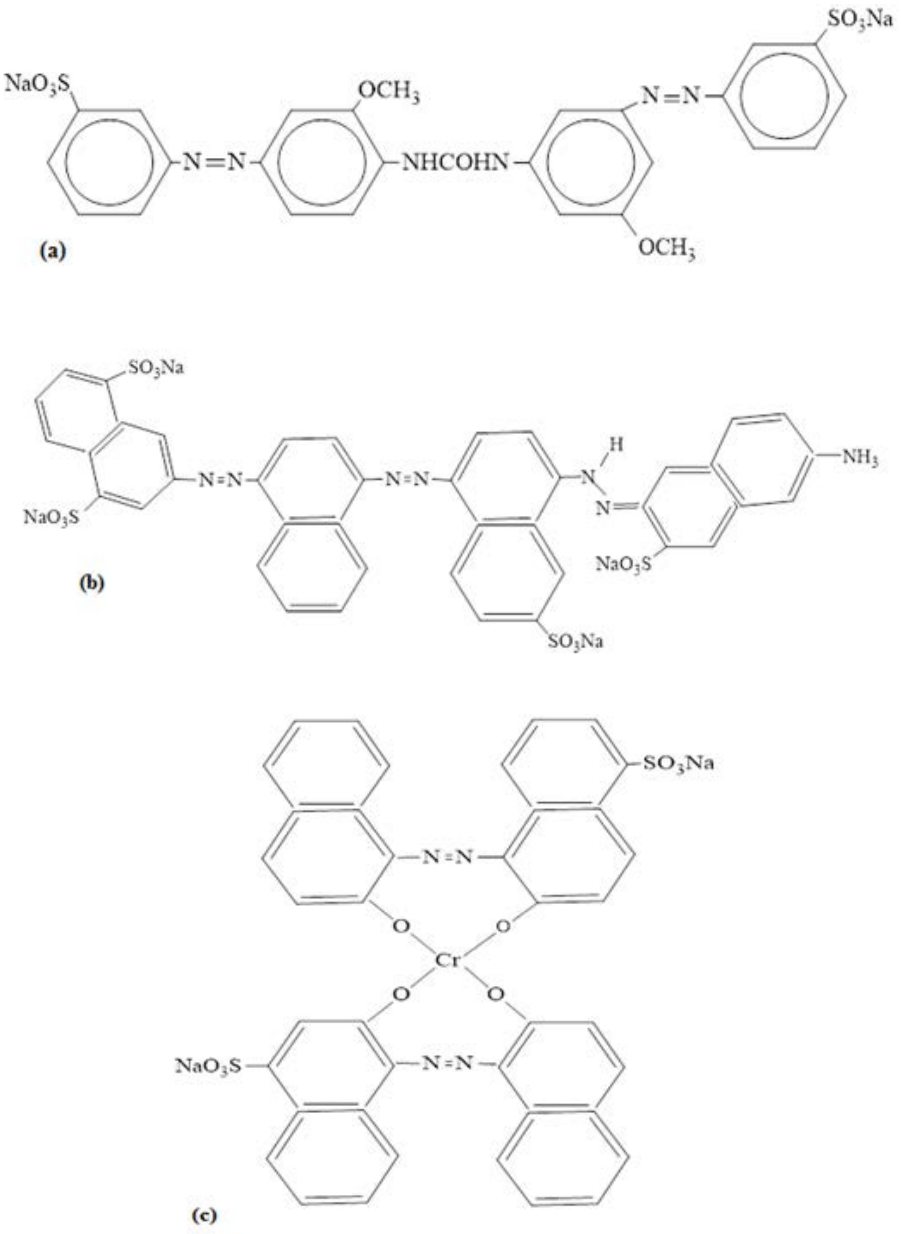

Fig. 1. Chemical structure of dyes: (a) direct yellow 132, (b) direct blue 71, and (c) acid blue 193.

in range from 10 to 100 mg/L were prepared by diluting the stock solution with distilled water.

MC material was collected from local market in Ho Chi Minh City, Vietnam. The raw clusters of charcoal were grounded and sieved to collect a fraction of 0.20–0.45 mm for experiments, labeled as MC. The MC material was treated further by forming slurry of 10 g of MC with 10 mL of 0.5 M H_3PO_4 solution, then irradiated for 5 min in an 800-W household microwave oven. The irradiated sample was cooled to room temperature, then filtered, washed with distilled water until pH of the filtrate was at 6.0–6.5, then dried in an oven at 100°C for 3 h to collect a final modified material as modified mangrove charcoal (MMC). Both MC and MMC materials were characterized by X-ray diffraction (XRD) spectroscopy, Fourier-transform infrared spectroscopy (FTIR), scanning electron microscope (SEM), and Brunauer–Emmett–Teller (BET) method. The pH_{zpc} of the MC and MMC was determined by the batch equilibrium method in 0.01 M NaCl [17].

2.2. Adsorption experiments

The batch adsorption experiments were conducted for each type of dyes to determine the effects of various factors including contact time, pH, adsorbent dosage, and initial concentrations of dyes on the sorption ability of MMC. All the experiments were performed at temperature of 30°C ± 1°C by mixing 0.2 g of MMC with 100 mL of each dye solution at specific concentration in flasks at 250 rpm. The adsorption mixture was then filtered through a fiberglass paper (0.45 μm) to collect samples for residue dye concentration analysis using UV visible spectrophotometry.

3. Results and discussion

3.1. Characteristics of adsorbent

Fig. 2 presents the SEM images of the MC and MMC, highlighting the differences of their surface morphologies. More openings, holes, and cave types, observed on the surface of the MMC, indicate the effectiveness of the microwave treatment using diluted phosphoric acid process in increasing the surface are which, in general, enhances the adsorption properties. As shown in Table 1, the BET surface area is 0.919 m^2/g in MC increased more than 100 times to 124.5 m^2/g in MMC. This shows that the combination of H_3PO_4 acid and microwave heating treatment process can remove effectively all organic residue in the original MC material, and also the MC framework can provide very high surface area material. The pH_{zpc} values of MC and MMC are 4.21 and 5.75, respectively (Table 1). This suggests that in acidic conditions, the adsorption of direct dyes on MMC is more favorable because of direct dye anion forms can be easily adsorbed on the MMC surface by the electrostatic attraction force.

Fig. 3 shows the XRD pattern of MC and MMC materials, which are both amorphous in nature. This is supported from the presence of a broad peak between 22° and 24° in both XRDs of the MC and MMC.

Fig. 4 shows FTIR spectra of MC, MMC, and dye-loaded MMC. In general, FTIR spectra of MC and MMC have fairly similar FTIR spectroscopic with some differences in features

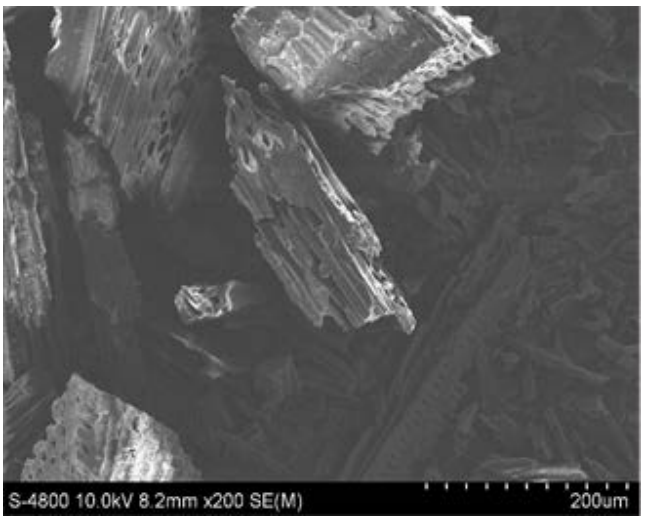

(a)

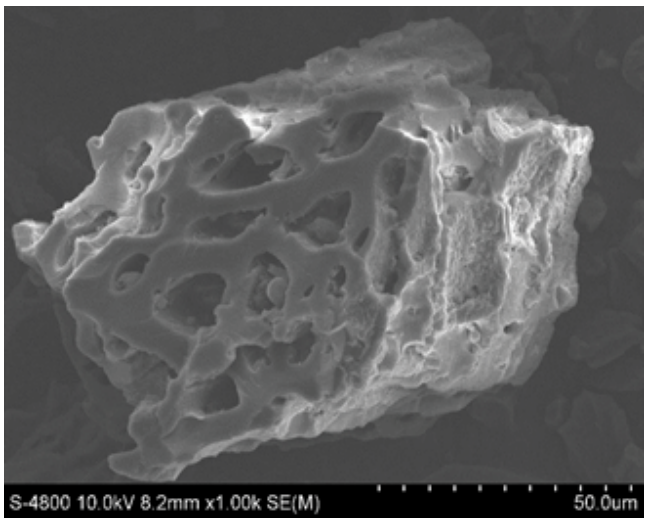

(b)

Fig. 2. SEM images of (a) MC and (b) MMC.

Table 1
BET surface area, pore volumes of MC and MMC

Materials	BET surface area (m^2/g)	Langmuir surface area (m^2/g)	pH_{zpc}
MC	0.919	5.71	4.21
MMC	124.46	146.9	5.75

and in intensity, suggesting some chemical changes on the surface resulted from microwave acid treatment. Several different functional groups can be identified. For example, the broad band observed in the region of 3,500–3,300 and 1,250–1,000 cm^{-1} assigned to –OH groups, peaks at 1,552 and 1,571 cm^{-1} assigned to C=O stretching band, and peak at 1,500 cm^{-1} of C=C double bond in alkenes are shown in

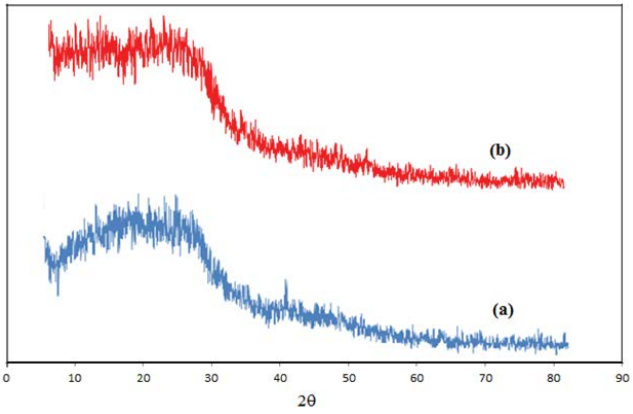

Fig. 3. XRD spectra of (a) MC and (b) MMC.

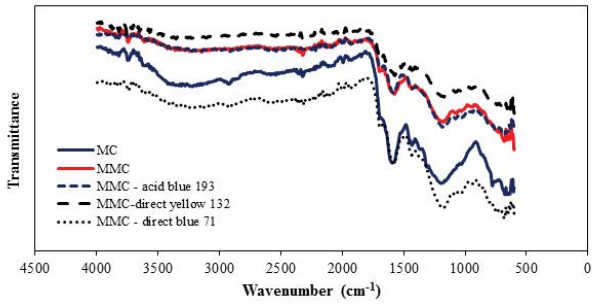

Fig. 4. FTIR spectra of MC, MMC and direct dyes loaded MMC.

both material. The absorption peaks at 2,850–2,920 cm^{-1} of CH stretching vibration and CH_2 asymmetrical vibrations are more distinctive in MC than in MMC. The lesser peak intensity observed in FTIR spectra of MMC than those of MC indicate less amount of organic residue on the surface; further support the effectiveness of the treatment with H_3PO_4 acid and microwave irradiation. Similar result was reported in literature for activated carbon material from apple waste after treatment using microwave and phosphoric acid [18]. For the FTIR spectra of the dye-loaded MMC (MMC-direct yellow 132, MMC-direct blue 71, and MMC-acid blue 193), it could be observed that the absorbance peaks at 1,137 cm^{-1} assassinated to CO groups stretching in alcohol or hydroxyl groups shifted to lower the wavenumber of spectra for all three direct dyes. These results indicated that functional groups on the MMC surface were affected by the adsorption of these dyes. A similar phenomenon was also observed for adsorption reactive dyes on activated carbon [19].

3.2. Effect of pH on the adsorption process

pH is one of the several important parameters in the adsorption process of direct dyes onto the MMC surface. Direct dyes are anionic, so that, the charge of the adsorbent surface, controlled via the pH value of the solution, will affect the magnitude of the adsorption. As mentioned in section 2.1, the pH_{zpc} of MMC was at 5.75, meaning that at pH less than 5.75, the adsorbent surface will be positive charge, thus, enhancing the adsorption of direct dyes via electrostatic attraction force. As shown in Fig. 5, the maximum adsorption

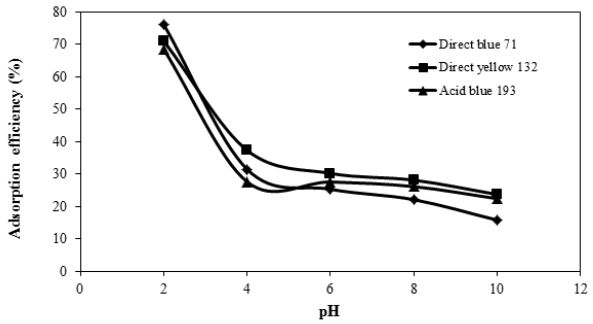

Fig. 5. Effect of pH on the adsorption of direct dyes onto MMC at 303 K.

efficiency (%) of all three types of direct dye was observed at pH 2.3. Increase in pH resulted in lower adsorption efficiency to a low plateau of 10%–25% at pH ≥ 6.

3.3. Adsorption kinetics

Based on previous data, pH 2.3 and temperature of 30°C ± 1°C was selected for further evaluation effect of other factors including initial concentration of the direct dyes and adsorbent dose (Figs. 6 and 7). It was observed that the adsorption rate was reduced with increasing the initial concentration of dyes from 10 to 30 mg/L, probably because a simple transportation limitation of more dye ions to available active sites on adsorbent surface. The higher the concentration, the slower the diffusion rate occurs, thus, reducing the adsorption rate. The adsorption rate, on the other hand, increased with increasing the adsorbent dose from 2.0 to 10.0 g/L at a fixed initial dye concentration, resulting from more available active sites in the process. Further increasing adsorbent dose beyond this point at the same dye concentrations will not effectively increase the removal process.

Two kinetic models, including the pseudo-first-order model and the pseudo-second-order model [20–23], were used to evaluate the experimental data and describe the adsorption process of dyes onto MMC. The pseudo-first-order model is as follows:

$$\frac{1}{q_t} = \left(\frac{k_1}{q_1}\right)\left(\frac{1}{t}\right) + \frac{1}{q_1} \tag{1}$$

where k_1 is the rate constant (min^{-1}); q_1 and q_t are the equilibrium adsorption capacity and the adsorption capacity (mg/g) at time t, respectively.

The pseudo-second-order model is as follows:

$$\frac{1}{q_t} = \frac{1}{k_2 q_2^2} + \frac{1}{q_2} t \tag{2}$$

where q_1 and q_2 are the equilibrium adsorption capacity (mg/g) and the adsorption capacity at time t, respectively; k_2 is the rate constant (g/mg min).

The intraparticle diffusion model is expressed as in Eq. (3):

$$q_t = k_p t^{0.5} + C \tag{3}$$

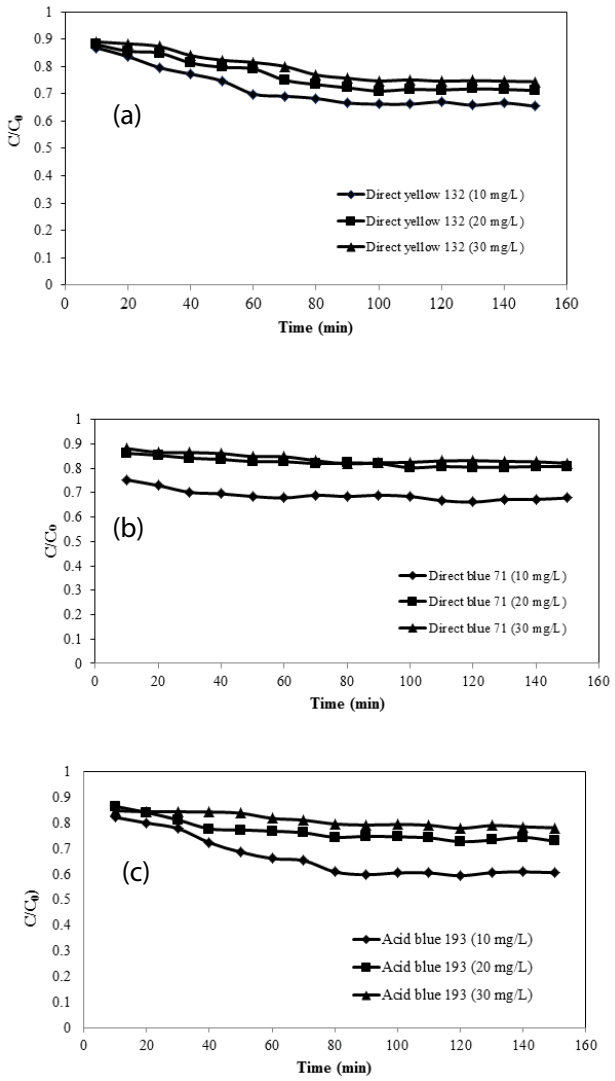

Fig. 6. Effect of contact time on the adsorption of direct dyes onto MMC at 303 K: (a) direct yellow 132, (b) direct blue 71, and (c) acid blue 193.

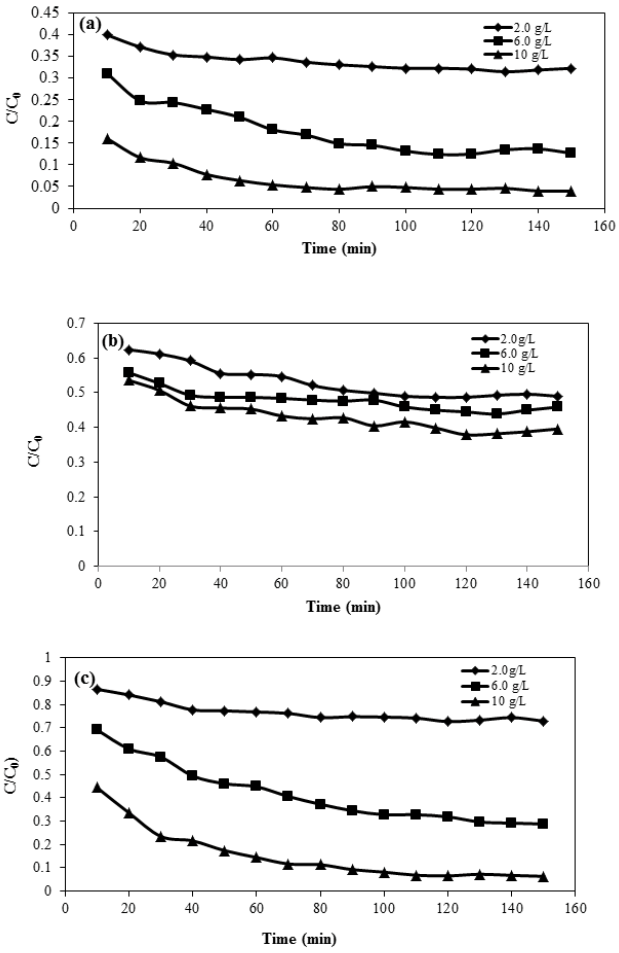

Fig. 7. Effect of adsorbent dosage on the adsorption of direct dyes onto MMC at 303 K: (a) direct yellow 132, (b) direct blue 71, and (c) acid blue 193.

where k_p is the intraparticle diffusion constant (mg/(g min$^{0.5}$) and C is a constant.

Parameters in Eqs. (1) and (2), including k_1, q_1, k_2, q_2, can be determined from the slope and intercept of their respective plots of $1/q_t$ versus $1/t$ and t/q_t versus t. The parameters of both kinetic models for the adsorption process of direct dyes onto MMC are shown in Table 2. The correlation coefficients of direct dyes for pseudo-second-order kinetic model were found to be higher than those obtained from the pseudo-first-order model, indicating that, the pseudo-second-order kinetic model appears to be a better description of the adsorption process of direct dyes on MMC. Figs. 8(a)–(c) shows the intraparticle diffusion model for adsorption of direct yellow 132, direct blue 71, and acid blue 193, respectively, onto MMC. The plots show three different parts that indicates the diffusion stages of direct dyes from liquid phase on the surface of MMC. In the first stage (the first line of the plot), direct dyes transfer on the external surface of the MMC. The second stage (intermediate line) is the intraparticle diffusion and the third stage is the equilibrium stage where the intraparticle diffusion begins at slowing down with very low values of the intraparticle diffusion constant, k_p (Table 3) due to extremely low solute concentrations in the solution and saturation of the material sites. For acid blue 193, the boundary between the second and third states is not very clear with k_p values for these stages were found to be 0.006 mg/g/min$^{0.5}$ at initial concentration of 10 and 20 mg/L and from 0.01 to 0.001 mg/g/min$^{0.5}$ at 30 mg/L. Thus, the third stage for direct yellow 132, direct blue 71, and second stage for acid blue 193 can be considered the rate-controlling step adsorption process of direct dyes onto MMC [19].

3.4. Equilibrium and thermodynamic adsorption

The adsorption of direct dyes on MMC material at 303, 313, and 323 K was conducted at initial concentration range from 10 to 150 mg/L at pH 2.3 and 100 min of contact time. The Langmuir and Freundlich models were used to describe the adsorption equilibrium [18,24–26].

Table 2
Kinetic parameters for adsorption of direct dyes onto MMC at 303 K

C_0 (mg/L)	Pseudo-first-order model			Pseudo-second-order model		
	k_1 (L/min)	q_1 (mg/g)	R^2	k_2 (g/mg/min)	q_2 (mg/g)	R^2
Direct yellow 132						
10	21.0	1.91	0.945	0.052	1.392	0.980
20	17.6	3.00	0.863	0.044	1.820	0.967
30	16.8	3.86	0.789	0.039	2.118	0.958
Direct blue 71						
10	3.70	1.67	0.927	0.311	1.290	0.998
20	4.76	1.93	0.838	0.149	1.418	0.996
30	5.72	2.65	0.812	0.144	1.655	0.993
Acid blue 193						
10	–3.45	0.302	0.703	0.045	0.291	0.998
20	12.0	0.283	0.949	0.091	0.533	0.992
30	4.98	3.09	0.567	0.090	1.86	0.988

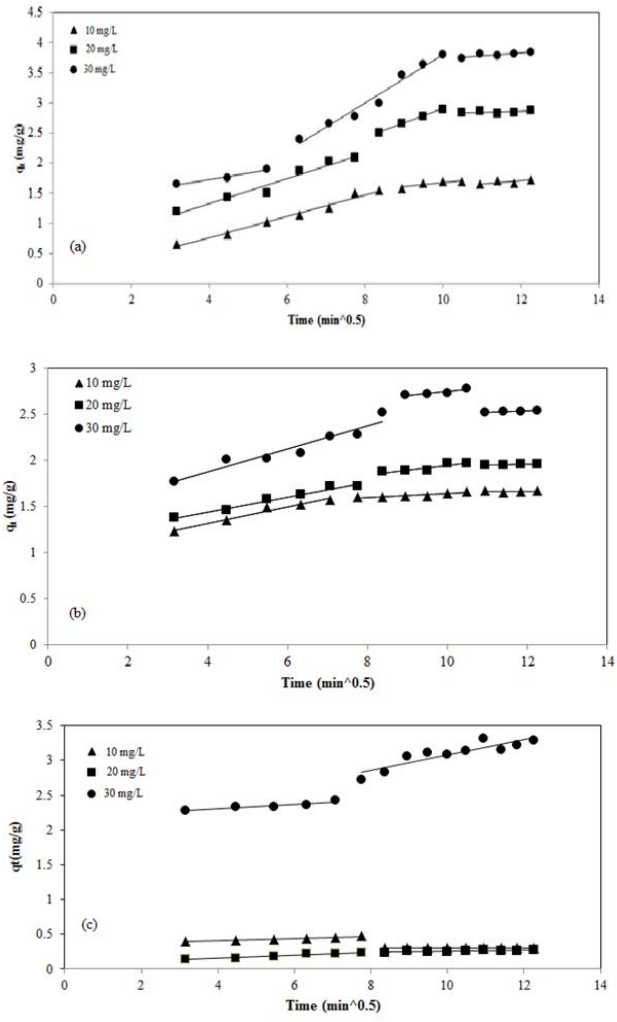

Fig. 8. Plots of intraparticle diffusion model for adsorption of (a) direct yellow 132, (b) direct blue 71, and (c) acid blue 193 onto MMC at 303 K.

The Langmuir model is expressed as in Eq. (4):

$$q_e = \frac{K_L q_m C_e}{1 + K_L C_e} \tag{4}$$

where C_e is the metal ion concentration in solution at equilibrium (mg/L); q_e is the amount of adsorbed metal ions per unit of adsorbent (mg/g); and K_L is Langmuir isotherm constant (L/mg) related to the theoretical maximum adsorption capacity q_m (mg/g) and energy of adsorption.

The Freundlich model is expressed by:

$$q_e = K_F C_e^{1/n} \tag{5}$$

where C_e is the metal ion concentration in solution at equilibrium (mg/L); q_e is the amount of adsorbed metal ions per unit of adsorbent (mg/g); n is the constant that related to adsorption intensity; and K_F is the Freundlich isotherm constant related to adsorption capacity.

Parameters of isotherm models were determined by nonlinear optimization technique to generate the residual root mean square error (RMSE) to evaluate the overall match between the experimental data and model prediction.

The plots of the nonlinear isotherm models from Eqs. (4) and (5) of the direct dyes adsorption process on MMC material at 303 K are shown in Fig. 9. Results from experiments at other temperatures are not included here. Calculated parameters of Langmuir and Freundlich models (Eqs. (4) and (5)) are summarized in Table 4.

As shown in Table 4, the calculated RMSE values suggest that the experimental data fits probably better with Freundlich isotherm model for three types of direct dyes, indicating that this adsorption process mostly involves heterogeneous surface of adsorbent and monolayer adsorption. Langmuir model calculated shows that the maximum capacity values, q_{max}, for the binding of direct dyes onto MMC followed a decreasing sequence of direct yellow 132 > direct blue 71 > acid blue 193, probably due to the differences in molecular structure of

Table 3
Intraparticle diffusion model parameters for adsorption of direct dyes onto MMC at 303 K

C_0 (mg/L)	Stage 1			Stage 2			Stage3		
	k_{p1} (mg/g/min$^{0.5}$)	C	R^2	k_{p2} (mg/g/min$^{0.5}$)	C	R^2	k_{p3} (mg/g/min$^{1/2}$)	C	R^2
Direct yellow 132									
10	0.199	0.054	0.982	0.066	1.107	0.766	0.046	1.15	0.500
20	0.207	0.509	0.960	0.243	0.476	0.997	0.013	2.69	0.16
30	0.180	1.29	0.968	0.399	0.200	0.969	0.048	3.25	0.704
Direct blue 71									
10	0.089	0.962	0.972	0.020	1.435	0.776	0.002	1.63	0.014
20	0.081	1.13	0.976	0.048	1.463	0.805	0.013	1.80	0.826
30	0.125	1.37	0.704	0.040	2.34	0.822	0.014	2.36	0.900
Acid blue 193									
10	0.015	0.347	0.94	0.006	0.192	0.606	0.006	0.190	0.616
20	0.023	0.062	0.957	0.006	0.062	0.612	0.006	0.077	0.611
30	0.032	2.179	0.841	0.010	1.980	0.798	0.001	0.186	0.687

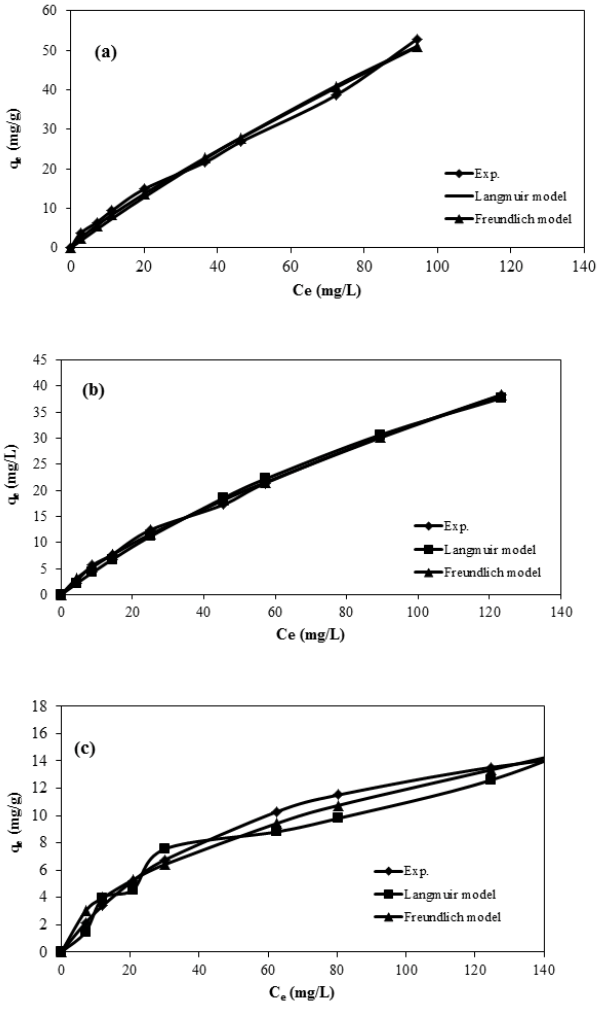

Fig. 9. Adsorption isotherm models of dyes onto MMC at 300 K: (a) direct yellow 132, (b) direct blue 71, and (c) acid blue 193.

each direct dyes [27]. In general, larger dyes, direct blue 71 (MW = 1,029.87 g/mol), lower diffusivity from the solution onto the adsorbent surface than that of smaller dyes, that is, direct yellow 132 (MW = 684.61 g/mol). However, this explanation does not fit well for acid blue 193, which has lowest maximum capacity even its molecular weight is also smallest (MW = 468.3785 g/mol). This could indicate that the adsorption process of acid blue 193 can involve specific chemical interaction with available function groups and its affinity with adsorbent surface. It was found that the maximum adsorption capacity, q_{max}, of MMC for direct dyes was equally much higher than those of other adsorbents reported, such as activated carbon prepared from shell of hazelnut adsorption of direct blue 71 [28], polyethyleneimine-treated peanut husk biomass for removal of direct dyes from aqueous solution [29], and bioadsorbent prepared from wheat bran for adsorption of reactive dyes by Sulak and Yatmaz [30].

In order to evaluate thermodynamic parameters of the adsorption process such as Gibbs free energy (ΔG) [25,26]:

$$\Delta G = -RT \ln K_d \tag{6}$$

where ΔG is Gibbs free energy change (kJ/mol), K_d is the equilibrium constant; T is solution temperature (K); and R is the gas constant (8.314 J/mol K).

The values of the equilibrium adsorption constant (K_d) can be calculated from the following equation:

$$K_d = \frac{\text{dye concentration in the solid phase at equilibrium (mg/g)}}{\text{dye concentration in liquid phase at equilibrium (mg/mL)}} \tag{7}$$

The enthalpy change, ΔH (kJ/mol) and entropy change, ΔS (J/mol K) of adsorption were calculated from the slope and intercept of the plot of $\ln(K_d)$ versus $1/T$ according to the van't Hoff equation at different adsorption temperature:

Table 4
Isotherm parameters of the adsorption process of direct dyes onto MMC

Temperature (K)	Langmuir model			Freundlich model		
	K_L (L/g)	q_{max} (mg/g)	RMSE	K_F ((mg/g)(mg/L)^n)	n	RMSE
Direct yellow 132						
303	0.03	258	1.817	1.07	1.18	1.03
313	0.004	148	1.538	1.23	1.27	0.637
323	0.006	120	0.777	1.31	1.30	0.646
Direct blue 71						
303	0.048	95.1	0.538	1.04	1.34	0.126
313	0.006	89.5	0.535	1.14	1.137	0.073
323	0.005	92.3	1.175	1.30	1.39	0.31
Acid blue 193						
303	0.017	19.9	1.52	1.08	1.91	1.32
313	0.016	20.9	0.241	1.14	1.93	0.221
323	0.015	22.9	0.119	1.17	1.89	0.09

Table 5
Thermodynamic parameters of the adsorption process of direct dyes onto MMC

T (K)	Direct yellow 132			Direct blue 71			Acid blue 193		
	ΔH (kJ/mol)	ΔS (J/mol K)	ΔG (kJ/mol)	ΔH (kJ/mol)	ΔS (J/mol K)	ΔG (kJ/mol)	ΔH (J/mol)	ΔS (J/mol K)	ΔG (kJ/mol)
303	8.36	28.3	–0.206	9.31	30.9	–0.078	3.45	12.0	–0.198
313			–0.489			–0.388			–0.318
323			–0.772			–0.697			–0.439

$$\ln K_d = \frac{\Delta S}{R} - \frac{\Delta H}{RT} \quad (8)$$

The values of ΔG, ΔH, and ΔS obtained in this study for direct dyes-loaded MMC are given in Table 5. In general, the results reveal that in the range of temperature from 303 to 323 K, the thermodynamic parameters favor for direct dyes adsorption. The negative values of ΔG confirmed the spontaneous nature of the adsorption process. The enthalpy change (ΔH) is positive for all direct dyes indicating the endothermic nature of the adsorption process. The positive values of entropy change (ΔS) reflect the affinity of MMC for direct dyes and suggest increased randomness at the adsorbent surface during the adsorption.

As shown in Table 4, the maximum adsorption capacity, q_{max}, of MMC for direct yellow 132 and direct blue 71 decreased at higher temperatures, while q_{max} for acid blue slightly increased at the same range of temperatures, which indicates the nature of the adsorption process. For the adsorption process of three dyes onto MMC, physical adsorption and chemisorption can be classified by the magnitude of enthalpy change. It suggested that enthalpy change <84 kJ/mol are typically those of physical adsorption type and enthalpy change of chemisorption type can range more than from 84 to 420 kJ/mol [19]. As seen in Table 5, the values of enthalpy calculated from Eq. (8) were +8.36, +9.31, and 3.45 kJ/mol for direct yellow 132, direct blue 71, and acid blue 193, respectively. This means that the adsorption process of direct dyes onto MMC is physical process. On the other hand, the values of entropy change, ΔS, included in Table 5 at different temperatures of direct yellow 132 (28.3 kJ/mol K) and direct blue 71 (30.9 J/mol K) are greater than that of acid blue 193 (12.0 J/mol K). This phenomenon is due to the decreasing randomness of the adsorption at solid–liquid interface for acid blue 193, leading to reduce adsorption capacity for this direct dye.

3.5. Regeneration of MMC

According to the results obtained in the study of pH on the adsorption of direct dyes onto MMC, the method solvent washing at high pH value for regeneration of MMC saturated with direct dyes was used. In this method, the solution of 0.1 M NaOH (pH 13) was used to remove residue of direct dyes from MMC, then washed with distilled water until pH 5 of elution. The resulting MMC was dried in the oven at 80°C for 24 h. The adsorption process of the treated MMC for direct dyes was repeated as mentioned above with batch adsorption conditions for each cycle, including 0.5 g of the regenerated MMC, 200 mg/L of initial concentration of direct dyes, pH 2.3 of the adsorption solution and 100 min contact time. The results of three regeneration cycles for the exhausted MMC are shown in Table 6. As seen in the results, it was found that the adsorption efficiency (%) for three direct dyes of the regenerated MMC in three cycles was only slightly changed. This can be concluded that MMC can be used multiple times for removal of direct dyes from aqueous solution.

3.6. Design of single stage batch adsorption system

Objective of single stage batch adsorption design is to treat a volume (L) of wastewater containing dye pollutant concentration, C_0, which is to be reduced to concentration C_t at time t. A simplified scheme of this is shown in Fig. 10. In general, an amount of adsorbent, m, is added to the adsorption solution; then at equilibrium condition, C_t will become to C_e, and the pollutant concentration on the solid phase changes from q_0 to q_e.

The mass balance of the system is described by Kumar and Porkodi [31]:

$$V_{C_0} - V_{C_e} = m_{q_e} + m_{q_0} \tag{9}$$

where V is volume of the adsorption solution (L); C_0 is the initial concentration of direct dyes (mg/L); m is the mass of adsorbent (g); C_e is the concentration of direct dyes at equilibrium (mg/L); q_0 is the adsorption capacity (mg/g), at time $t = 0$, $q_0 = 0$; and q_e is the adsorption capacity at equilibrium time.

As shown in adsorption equilibrium studies, Freundlich model was better fit to the experimental equilibrium data for all direct dyes; its equation was used to predict the amount of direct dyes required to remove a certain percentage of direct dyes from specific volume of solution. Rearrange of Eq. (7) gives adsorbent/solution ratio for this particular system:

$$\frac{m}{V} = \frac{C_0 - C_e}{K_F \left(C_e\right)^{1/n}} \tag{10}$$

Fig. 11 shows the plot of predicted amounts of MMC for direct dyes removal at different solution volume at initial concentrations of 30 mg/L for 90%, 95%, and 99.9% removal at 30°C. According to data shown in the plots, the removal of 99% direct dyes from 20 m^3 solution would require MMC at 6.2 kg for direct yellow 132, 5.7 kg for direct blue 71, and 7.5 kg for acid blue 193. These data could be useful in selecting

Table 6
Regeneration of MMC saturated with direct dyes

Regeneration cycle	Efficiency (%)		
	Direct yellow 132	Direct blue 71	Acid blue 193
1	98.2	96.7	90.8
2	97.8	96.5	90.4
3	98.0	96.3	89.7

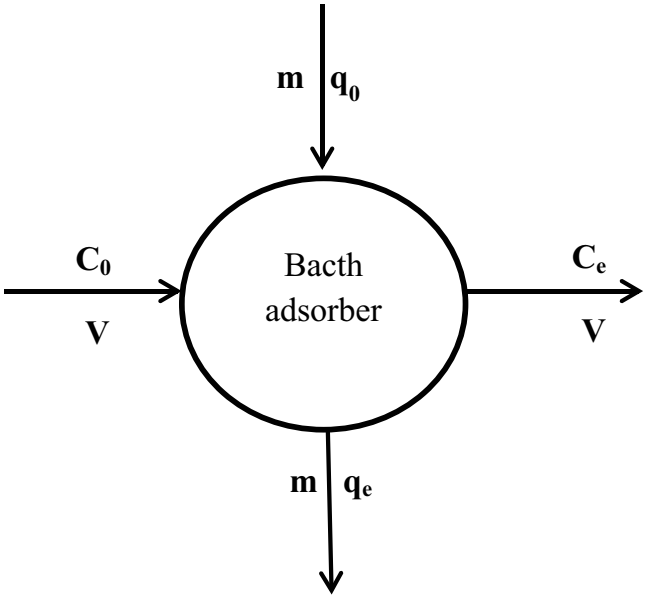

Fig. 10. Schematic representation of the single stage batch adsorption system.

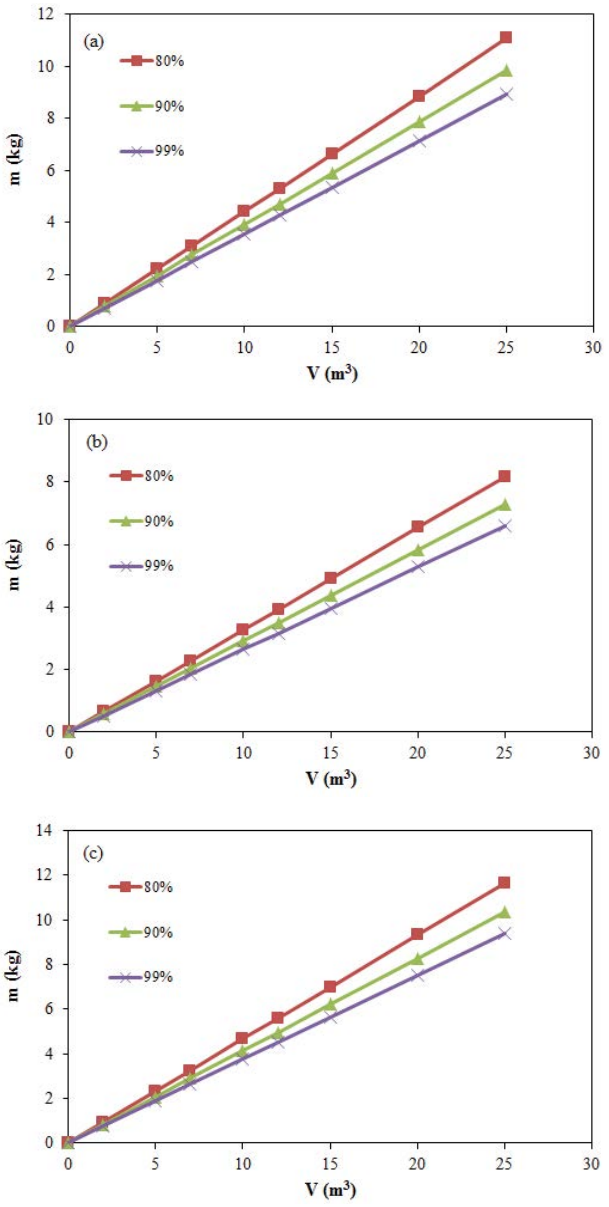

Fig. 11. Plots for prediction of the amounts of MMC for direct dye removal at different solution volume (a) direct yellow 132, (b) direct blue 71, and (c) acid blue 193.

batch adsorption systems to achieve specific removal efficiency of direct dyes in wastewater.

4. Conclusion

This study presents a high adsorption capacity of the MMC for adsorption of direct dyes using a simple and effective treatment with phosphoric acid in a conventional household microwave oven. At pH 2.3 and 100 min contact time, it was found that the maximum capacity values, q_{max}, for the binding of direct dyes onto MMC followed a decreasing sequence of direct yellow 132 > direct blue 71 > acid blue 193. The adsorption capacity of experimental data was used to calculate the amount of adsorbent need in one-stage batch adsorption system to achieve specific removal efficiency; this calculation could be useful for selecting batch adsorption system for removal of direct dyes from wastewater in each specific application.

Acknowledgment

The author would like to thank Mr. Ho Thanh Nguyen and Ms. Vo Thi Hong Nhung for the help and co-operation needed to complete the experiments in this work.

References

[1] H.T. Vu, L.C. Pham, A dynamic approach to assess international competitiveness of Vietnam's garment and textile industry, Springer Plus, 5 (2016) 2–13.
[2] M. Riera-Torres, C. Gutiérrez-Bouzán, M.Crespi, Combination of coagulation-flocculation and nanofiltration techniques for dye removal and water reuse in textile effluent, Desalination, 253 (2010) 53–59.
[3] A. Mishra, M. Bajpai, The flocculation performance of Tamanrindus mucilage in relation to removal of vat and direct dyes, Bioresour. Technol., 97 (2006) 1055–1059.
[4] M.R. Gadekar, M.M. Ahammed, Coagulation/flocculation process for dye removal using water treatment residual: modelling through artificial neutron networks, Desal. Wat. Treat., 57 (2016) 26392–26400.
[5] A. Pirkarami, M.E. Olya, Removal of dye from industrial wastewater with an emphasis on improving economic efficiency and degradation mechanism, J. Saudi Chem. Soc., 21 (2015) 179–186.
[6] A. Dalvand, M. Gholami, A. Joneidi, N.M. Mahmoodi, Dye removal, energy consumption and operating cost of electrocoagulation of textile wastewater as a clean process, Clean Soil Air Water, 39 (2011) 665–672.
[7] J. Vidal, L. Villegas, J.M. Peralta-Hernández, R.S. Gonzallez, Removal of acid black 194 dye from water by electrocoagulation with aluminum anode, J. Environ. Sci. Health, Part A, 51 (2016) 289–296.
[8] H.R. Rashidi, N.M.N. Sulaiman, N.A. Hasgim, C.R.C. Hassan, M.R. Ramli, Synthetic reactive dye wastewater treatment by using nano-membrane filtration, Desal. Wat. Treat., 55 (2015) 86–95.
[9] C. Thamaraiselvan, U.M. Noel, Membrane processes for dye wastewater treatment: recent progress in fouling control, Crit. Rev. Environ. Sci. Technol., 45 (2015) 1007-1049.
[10] K. Santhy, P. Selvapathy, Removal of reactive dyes from wastewater by adsorption on coir pith activated carbon, Bioresour. Technol., 97 (2006) 1329-1336.
[11] V.V.B. Rao, S.M. Rao, Adsorption studies on treatment of textile dye in industrial effluent by fly ash, J. Chem. Eng., 116 (2006) 77-84.
[12] A.M. Herrera-González, A.A. Peláez-Cid, M. Caldera-Villalobos, Adsorption of textile dyes present in aqueous solution and wastewater using polyelectrolytes derived from chitosan, J. Chem. Technol. Biotechnol., 92 (2017) 1488-1495.
[13] K.S. Bharathi, S.T. Ramesh, Removal of dyes using agriculture waste as low-cost adsorbents: a review, Appl. Water Sci., 3 (2013) 773-790.
[14] O.S. Bello, K.A. Adegoke, A.A. Olaniyan, H. Abdulazeez, Dye adsorption using biomass wastes and natural adsorbents: overview and future prospects, Desal. Wat. Treat., 53 (2015) 1292-1315.
[15] A.P. Vieira, S.A.A. Santana, C.W.B. Bezerra, H.A.S. Silva, J.A.P. Chaves, J.C.P. de Melo, E.C. da Silva Filho, C. Airoldi, Kinetics and thermodynamics of textile dyes adsorption from aqueous solution using babassu coconut mesocarp, J. Hazard. Mater., 166 (2009) 1272-1278.
[16] M. Goswami, P. Phukan, Enhanced adsorption of cationic dyes using sulfonic acid modified activated carbon, J. Environ. Chem. Eng., 5 (2017) 3508-3517.
[17] J. Singh, N.S. Mishra, Uma, S. Banerjee, Y.C. Sharma, Comparative study of physical characteristics of raw and modified sawdust for their use as adsorbents for removal of acid dye, BioResources, 6 (2011) 2732–2743.
[18] R.H. Hesas, A.A. Niya, W.M.A.W. Daud, J.N. Sahu, Preparation and characterization of activated carbon from apple waste by microwave-assisted phosphoric acid activation: application in methylene blue adsorption, BioResources, 8 (2013) 2950-2966.
[19] Y.S. Aldegs, M.I. EI-Barghouthi, A.H. EI-Sheikh, G.M. Walker, Effect of solution pH, ionic strength, and temperature on the adsorption behavior of reactive dyes on activated carbon, Dyes Pigm., 77 (2008) 16-23.
[20] M.F. Hou, C.X. Ma, W.D. Zhang, X.Y. Tang, Y.N. Fan, H.F. Wan, Removal of rhodamine B using iron-pillare bentonite, J. Hazard. Mater., 186 (2011) 1118-1123.
[21] M. Arami, N.Y. Limaee, N.M. Mahmoodi, Evaluation of the adsorption kinetics and equilibrium for the potential removal of acid dyes using a biosorbent, J. Chem. Eng., 139 (2008) 2-10.
[22] R. Aravindhan, J.R. Rao, B.U. Nair, Kinetic and equilibrium studies on biosorption of basic blue dye by green macro algae *Caulerpa scalpelliformis*, J. Environ. Sci. Health, Part A, 42 (2007) 621-631.
[23] A.A. Babaei, S.N. Alavi, M. Akbarifar, K. Ahmadi, A.R. Esfahani, B. Kakavandi, Experimental and modeling study on adsorption of cationic methylene blue dyes onto mesoporous biochars prepare from agrowaste, Desal. Wat. Treat., 57 (2016) 27199-27212.
[24] A. Tabak, N. Baltas, B. Afsin, M. Emirik, B. Caglar, E. Eren, Adsorption of reactive red 120 from aqueous solution by cetylpyridinium-bentonite, J. Chem. Technol. Biotechnol., 85 (2010) 1199-1207.
[25] S. Banerjee, M.G. Dastidar, Use of jute processing wastes for treatment of wastewater contaminated with dye and other organics, Bioresour. Technol., 96 (2005) 1919-1928.
[26] D. Datta, Ö.K. Kuyumcu, Ş.S. Bayazit, M.A. Salam, Adsorptive removal of malachite green and rhodamine B dyes on Fe_3O_4/activated carbon composite, J. Dispersion Sci. Technol., 38 (2017) 1556-1562.
[27] R. Malarvizhi, Y.S. Ho, The influence of pH and the structure of the dye molecules on adsorption isotherm modeling using activate carbon, Desalination, 264 (2010) 97-101.
[28] Ö. Yavuz, A.H. Aydin, Removal of direct dyes from aqueous solution using various adsorbent, Pol. J. Environ. Stud., 15 (2006) 155-161.
[29] S. Sadaf, H.N. Bhatti, M. Arif, M. Amin, F. Nazar, Adsorptive removal of direct dyes by PEI-treated peanut husk biomass: Box-Behnken experimental design, J. Chem. Ecol., 31 (2015) 252-264.
[30] M.T. Sulak, H.C. Yatmaz, Removal of textile dyes from aqueous solution with eco-friendly biosorbent, Desal. Wat. Treat., 37 (2012) 169-177.
[31] K.V. Kumar, K. Porkodi, Batch adsorber design for different solution volume/adsorbent mass ratios using the experimental equilibrium data with fixed solution volume/adsorbent mass ratio of malachite green onto orange peel, Dyes Pigm., 74 (2007) 590-594.